Journal of Colloid and Interface Science 413 (2014) 8–16

Contents lists available at ScienceDirect

Journal of Colloid and Interface Science

www.elsevier.com/locate/jcis

Study of the particles' structure dependent rheological behavior for polymer nanospheres based shear thickening fluid

Wanquan Jiang [a,*], Fang Ye [a], Qianyun He [b], Xinglong Gong [b,*], Jiabin Feng [b], Lei Lu [b], Shouhu Xuan [b,*]

[a] Department of Chemistry, University of Science and Technology of China (USTC), Hefei 230026, PR China
[b] CAS Key Laboratory of Mechanical Behavior and Design of Materials, Department of Modern Mechanics, USTC, Hefei 230027, PR China

ARTICLE INFO

Article history:
Received 13 May 2013
Accepted 16 September 2013
Available online 21 September 2013

Keywords:
Shear thickening
Rheological properties
Poly(styrene–acrylic acid) nanospheres
Viscosity
Mechanism

ABSTRACT

A novel kind of shear thickening fluid (STF) was developed *via* dispersing poly(styrene–acrylic acid) (PS–AA) nanospheres into ethylene glycol (EG). By varying the structure characteristics of the PS–AA particles, STFs with different rheological properties can be obtained. Firstly, the influence of the styrene/acrylic acid ratio on the PS–AA nanospheres was investigated. It was found that the higher ratio often led to the better shear thickening (ST) effects and under the optimum condition the maximum viscosity of the STF could reach to 152 Pa s, while the ST effects decreased under further increasing the monomer ratio. Then, the divinyl benzene (DVB) was introduced to increase the cross-link density of the PS–AA. In comparison with the non-cross-link PS–AA nanospheres, the poly(styrene–acrylic acid–divinyl benzene) (PS–AA–DVB) based STFs exhibited much higher ST effects and the maximum viscosity was up to 385 Pa s when the DVB was only increased to 0.3%. In combination of the rheological properties and the structure characterization, a possible mechanism for the ST behavior was proposed and the influence of the particles' characteristics on the mechanical performance of the PS–AA based STF was carefully analyzed.

1. Introduction

When subjected to a strong impact, a liquid suspension with flowable behavior can become a solid like state with rigid behavior. This phenomenon was defined as shear thickening (ST) behavior, characterized by a pronounced increase in suspension viscosity when the shear rate reaches up to a critical value [1–3]. The liquid–solid phase transition is reversible, which means that the viscosity decreases immediately as soon as the shear rate decreases [3]. ST behavior initially attracted considerable interest due to its damage to process equipment and dramatic changes in suspensions microstructures, resulting in poor fluid and coating properties, which was believed to be a severe problem in industrial situations. The early investigations in ST behavior were to prevent this phenomenon for a given range of processing conditions or for specific applications. The STFs also have been utilized in many commercial applications including the ski boot cushioning, liquid coupling, shock absorber, rotary speed limiters, damping device, control devices, body armor [3–6], etc.

Based on their microstructure dependent macroscopic properties, two mechanisms order-to-disorder transition (ODT) and hydrocluster have been developed to analyze the ST behavior. Hoffman [1,2,7] firstly proposed the ODT mechanism and the ST was ascribed to a transition from an order two-dimensional structure (where the particles were ordered into layers) to a more random three-dimensional structure at a critical shear rate. This phenomenon had been experimentally demonstrated by small angle light scattering [1,8] and the small angle neutron scattering measurement [9]. However, several researchers have questioned whether an order–disorder transition was necessary for ST, and some papers [10,11] stated that the order structure was not always observed prior to the onset of ST. Therefore, order–disorder transition may accompany ST, but is not prerequisite for ST. The hydrocluster mechanism proposed that ST was a consequence of a shear-induced non-equilibrium and self-organization of the particles into stress-bearing particle clusters. This self-organized microstructure was owing to the dominance of short-range hydrodynamic lubrication forces [12], which has been proven by many experimental results including the rheo-optical experiment [13], stress-jump rheological measurements [14], neutron scattering [15,16]. Very recently, Cheng et al. [17] identified and visualized the hydroclusters as the origin of ST in colloidal suspensions by combining fast confocal microscopy with simultaneous force measurements. The Stokesian dynamics simulations also supported this mechanism [18,19], therefore the hydrocluster mechanism was accepted as the standard model to explain the ST phenomenon.

Rheological properties of STFs were highly dependent on the suspended phase, the solvent [20,21], and the additives [22–25],

* Corresponding authors. Fax: +86 551 63600419.
E-mail addresses: jiangwq@ustc.edu.cn (W. Jiang), gongxl@ustc.edu.cn (X. Gong), xuansh@ustc.edu.cn (S. Xuan).

0021-9797/$ - see front matter © 2013 Elsevier Inc. All rights reserved.
http://dx.doi.org/10.1016/j.jcis.2013.09.020

in which the suspended phase was the most important factor. Barnes [3] pointed that all suspensions of solid particles would exhibit the ST phenomenon given the right circumstances. To our knowledge, the particles for the STF can be divided into three categories. Firstly, the ST phenomenon was originated from many important industrial process including minerals processing and tailings disposal, the forming of ceramic components, pumping of coal–water mixtures, construction with concrete, and pharmaceutical production [24], thus the particles early studied by researchers were clay, quartz power, red iron oxide pigment, shale, limestone [3] and some inorganic particles such as silica [26,27], titania [28,29], calcium carbonate [30,31], alumina [32] and barium sulfate precipitated [33]. The second kind is the deformable particles such as blood cells [3], starch particles [34], wheat starch particles [35] and cornstarch particles [36]. The last kind is the man-made particles such as polyvinylchloride (PVC), poly(styrene–acrylonitrile) (PS–AN), polystyrene (PSt) [3], polymethylmethacrylate (PMMA) [20], poly(styrene–ethyl acrylate) (PS–EA) [37], carbon nanofibers [38], and the most popular silica particles for their easy preparation.

Due to the versatile molecular structures and surface properties, the polymer particles were very favorable in the STFs. Since the tunable hardness, charges, and elastic property, many polymer particles based STF exhibited strong ST behavior. The suspensions of 58 vol.% of PS–EA in EG exhibited a strong ST effect with a small initial viscosity under 10 Pa s at a static state but the maximum viscosity up to 10^4 Pa s at the transition in a steady shear test with a gap size of 800 μm [37]. However, the ST effect of the PMMA-STF was tender and more practical in the energy absorption under low intensity due to the low maximum viscosity in the ST region [20]. It was reported that the particle hardness exhibited great influence on the rheological properties of the STF which further affected the correlative STF-fabric performance [39,40]. Unfortunately, the detailed mechanism for this phenomenon was still expectative and the relative experimental evidences were needed. In the past decades, the influences of parameters of the particles such as the particle concentration [3,20], particle size [3,41], size distribution [28], sharp [42,30] and particle surface on the rheological properties of STFs (the onset of ST, the severity of ST, and the formation of hydrocluster) have been carefully studied. However, there has been comparatively little research into the influence of the inner structure of the suspended particles. Therefore, how about the particles' characteristics affected the ST behavior was emergent for understanding the essence of the ST behavior.

In this work, poly(styrene–acrylic acid) (PS–AA) nanospheres with different molecular structures were synthesized and dispersed into the EG solvent for the preparation of STF. The characteristics of the PS–AA nanospheres can be controlled by varying both the monomer molar ratio of styrene/acrylic acid and cross-linking reagent DVB. The rheological properties of these novel kind STFs were tested by using a rheometer and the particles' structure dependent ST behaviors was systematically investigated. Based on experimental results, a possible mechanism for the structural dependent ST behavior was proposed and the relative parameters were analyzed. This work was essential for developing new kind of STF system with better ST behavior, which further supplied novel understandings for the STF.

2. Experimental section

2.1. Materials

Acrylic acid (AA, Chemical Pure), Ethylene glycol (EG, analytical reagent), Potassium peroxydisulfate ($K_2S_2O_8$, analytical reagent), Sodium hydroxide (NaOH, analytical reagent), were used as received. Styrene (St, Chemical Pure), Divinyl benzene (DVB, Chemical Pure), were distilled under vacuum before being used. All the reagents were purchased from Sinopharm Chemical Reagent Co., Ltd. Twice-distilled water was used in the present study.

2.2. The preparation of PS–AA particles

All polymerizations were conducted in a 500-ml three-neck flask, which was fitted with a reflux condenser, a mechanical stirrer and a nitrogen inlet. Given amount of the monomers and distilled water were firstly added into the flask. The mixture was vigorously stirred at about 300 rpm for 30 min at room temperature, and then the $K_2S_2O_8$ was added as initiator. After 10 min, the reactor was heated up to 75 °C in a water bath and maintained for 6 h. The polymerization was conducted under nitrogen atmosphere and the resultants were collected by centrifugation after the polymerization. The particles were rinsed by distilled water for three times. At last, the obtained nanoparticles were dried under vacuum at 50 °C over night.

Five kinds of PS–AA particles with different monomer molar ratios of styrene/acrylic acid at a fixed amount of styrene and six kinds of PS–AA particles with different amounts of cross-linking monomer DVB were synthesized. The ratios of styrene/acrylic acid were 3/1, 5/1, 7/1, 8/1, 9/1 and the amount of cross-linking monomer DVB were 0.1%, 0.2%, 0.3%, 0.4%, 0.5%, 0.6% according to the styrene. For simplicity, the DVB cross-linked PS–AA was defined as PS–AA–DVB.

2.3. The preparation of PS–AA based STF

Typically, the STFs were prepared by adding a given amount of PS–AA particles or PS–AA–DVB particles directly into ethylene glycol. Then the mixtures were mixed for 24 h in a ball crusher so as to obtain a uniform distribution of polymer particles within the suspension and to insure the particles were not aggregated. At last, the samples were sonicated for an hour in order to remove the air bubbles.

2.4. Rheological measurements

Rheological measurements were carried out on a stress and strain controlled rheometer (Anton-Paar MCR301) at 25 °C with cone-plate geometry having a cone angle of 0.2° and a diameter of 25 mm. Both steady-shear and oscillatory-shear tests were conducted on each sample with a gap size of 0.05 mm to measure the STF rheology under both static and dynamic loading conditions. For steady-shear test, a pre-shear of 1 s^{-1} was applied for 60 s prior to further measurement to remove loading effects.

2.5. Characterization

The field emission scanning electron microscope (FE-SEM, 20 kV) images were taken on a JEOL JSM-6700F SEM. Transmission electron microscopy (TEM) photographs were taken on a JEM-2011 with an accelerating voltage of 200 kV TEM. Infrared (IR) spectra were recorded in the wavenumber range 4000–400 cm^{-1} with a Nicolet 8700 Fourier transform infrared (FT-IR) spectrometer using a KBr wafer.

3. Results and discussion

3.1. Preparation and characterization of the PS–AA nanospheres

The PS–AA nanospheres with different inner structures were obtained by soap-free emulsion polymerization. In this work, the

chemical components of the PS–AA nanospheres were turned through varying the molar ratio of styrene/acrylic acid. Fig. 1 represented the typical SEM and TEM images of as-prepared PS–AA nanospheres synthesized under the styrene/acrylic acid ratio of 7/1, 8/1 and 9/1, respectively. It can be seen that all the final products exhibited a spherical morphology with average diameter of about 330 ± 30 nm. These spherical nanoparticles were uniform and they could pack to form hexagonal structure on the copper plate, which can be clearly observed from the SEM images. All the PS–AA nanospheres synthesized under other ratios (3/1, 5/1) were also spherical and uniform (Fig. SI 1), which indicated the ratio exhibited few influence on the morphology of the PS–AA nanosphere. As a result, the PS–AA nanospheres with different inner structures were successfully achieved by varying the monomer ratio.

Besides the monomer ratio, the influence of the cross-linking reagent on the PS–AA nanospheres was also investigated. Keeping the other parameters as constant (the monomer ratio was 8), the cross-linking reagent varied from 0.1% to 0.6% was applied to synthesize PS–AA nanospheres. All the final products were monodisperse and had a narrow size distribution (Figs. 2 and SI 2). Fig. 2a and b show the SEM and TEM images of the PS–AA–DVB nanoparticles prepared by adding 0.3% DVB. Similar to the non-cross-linked PS–AA nanoparticles, the PS–AA–DVB nanoparticles also had a spherical structure. The further investigation of the SEM and TEM images indicates that the size and the shape of the final products were not dependent on the cross-linking reagent, thus all of them exhibited a similar morphology.

Due to the difference of the component, the inner structures of these PS–AA nanoparticles were variable. Fig. 3a shows the typical FT-IR spectra of PS–AA particles synthesized under the ratio of St/AA = 3/1. A wide absorption band between 3600 and 3300 cm^{-1} was found in the spectrum, which was assigned to the stretching vibrations of hydroxyl (–OH) in the carboxyl groups. The peaks at 1600, 1492, and 1452 cm^{-1} were attributed to the stretching vibration of benzene ring skeleton. The peak at 3050 cm^{-1} may be corresponded to the C–H stretching on the benzene ring. These absorption peaks indicated the existence of benzene ring groups on PS–AA particles. In addition, the peaks located at 2921 and 1705 cm^{-1} were attributed to the stretching vibrations of methylenes and carbonyl groups, respectively. With increasing of the St/AA ratio, the content of the carbonyl group in the final PS–AA nanospheres decreased, therefore the absorption of carbonyl groups at 1705 cm^{-1} sharply decreased when the St/AA ratio increased from

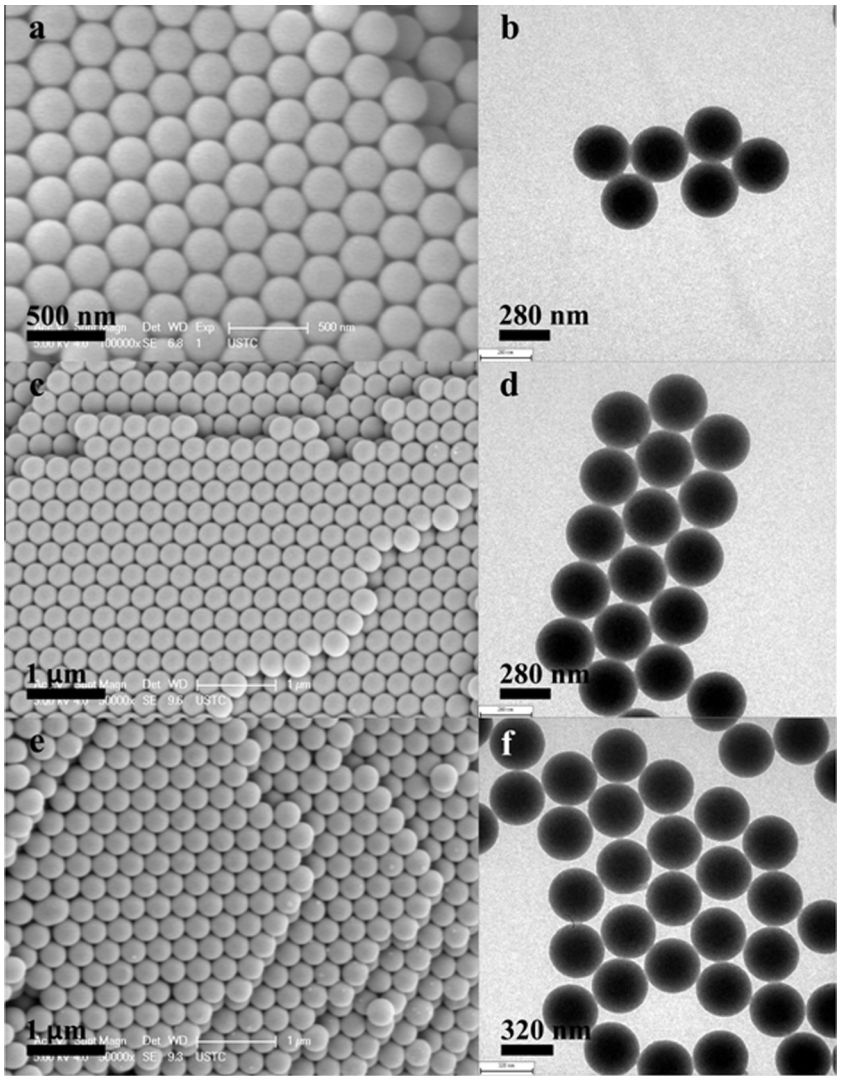

Fig. 1. SEM and TEM photographs of the obtained PS–AA particles synthesized with different monomer molar ratios of St/AA. St/AA = 7/1 (a and b), 8/1 (c and d) and 9/1 (e and f).

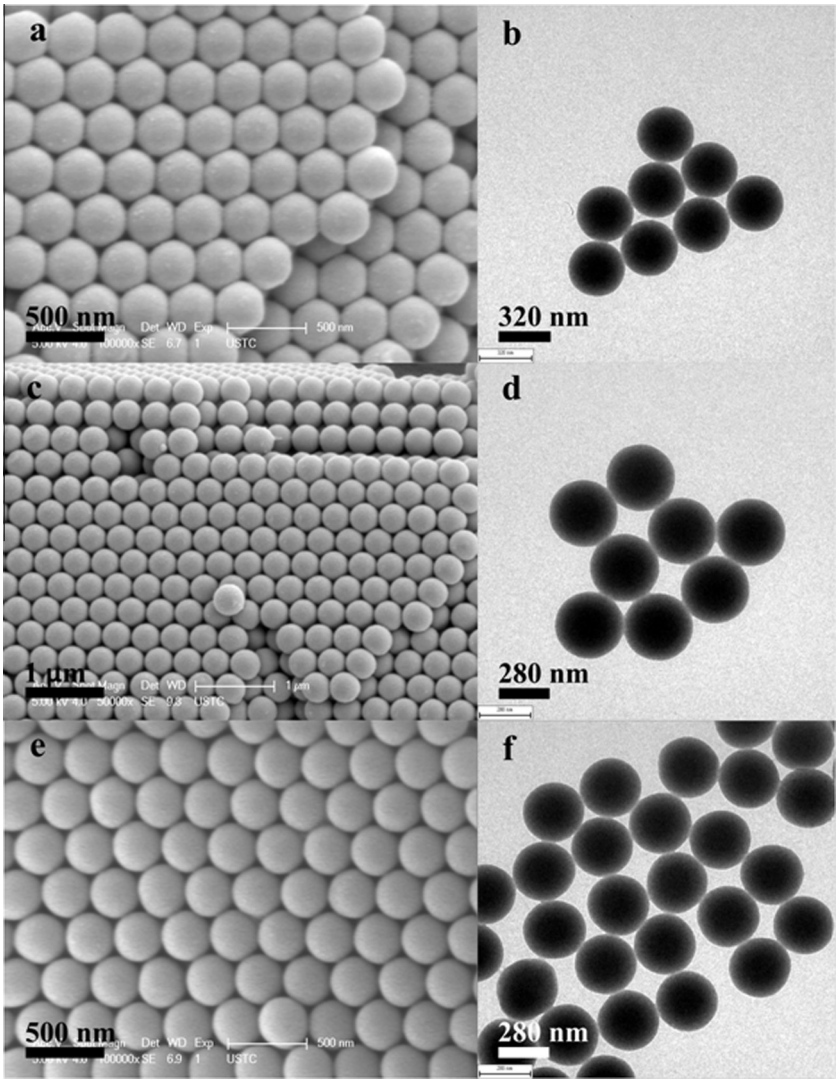

Fig. 2. SEM and TEM images of the obtained PS–AA particles synthesized with different amounts of cross-linking monomer DVB. 0.1% (a and b), 0.3% (c and d) and 0.5% (e and f).

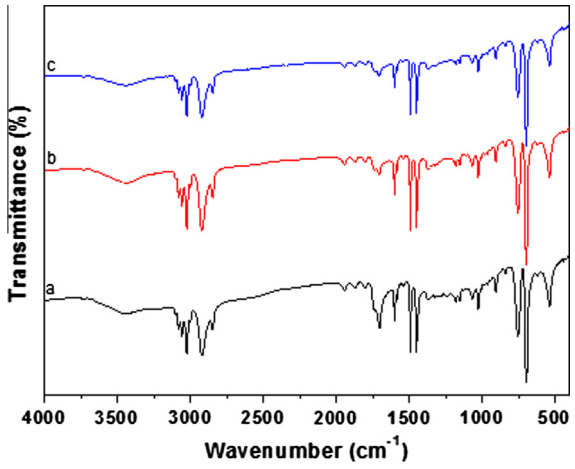

Fig. 3. FTIR spectra of the PS–AA particles with the ratio of St/AA = 3/1 (a), St/AA = 9/1 (b) and the amount of DVB = 0.3% (c).

3/1 to 9/1 (Fig. 3b). Since only a very little content of the DVB was used for the synthesis, the PS–AA–DVB exhibited a same FTIR spectrum (Fig. 3c) to the non-cross-linking one, although the structural characteristics have been strongly changed.

3.2. The ST rheology behavior of the PS–AA nanospheres based STF

By dispersing the above synthesized PS–AA nanospheres into the EG, the novel STF was obtained. Fig. 4a shows the static rheological properties of the PS–AA nanospheres based STFs for different particle concentrations, in which the dispersing nanoparticles were synthesized at a St/AA ratio of 7/1. It can be observed that each sample exhibited typical ST behavior and ST became severer with increased mass fraction, which agreed well with the previous results [3,4]. With increasing of the particles loading, the viscosity curve became steeper and the maximum viscosity in ST region increased. The shear rate for the onset of ST was also highly dependent on the mass fraction: the higher the concentration, the smaller the critical shear rate. It is well known that the particle concentration was one of the most important parameters controlling the ST behavior of suspensions. According to the hydrocluster mechanism, ST was a consequence of shear-induced non-equilibrium and self-organization of particles into stress-bearing particle clusters. At high concentration, the average distance between two adjacent particles would be shortened, the hydrodynamic force would be easier to move more particles to form larger particle clusters. Therefore, as the particle concentration increased, the critical shear rate decreased and ST behavior enhanced.

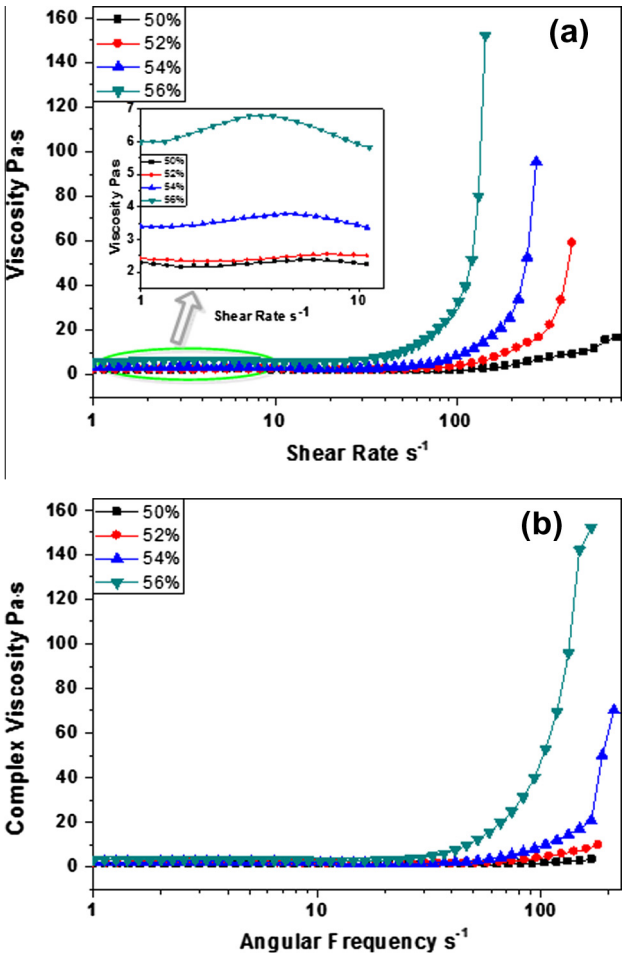

Fig. 4. (a) Viscosity *vs.* shear rate for different PS–AA mass fraction suspensions: 50%, 52%, 54%, 56% under steady shear mode. (b) Complex viscosity *vs.* angular frequency for different PS–AA mass fraction suspensions: 50%, 52%, 54%, 56%. Dynamic frequency sweep at $T = 25$ °C, $\gamma = 200\%$.

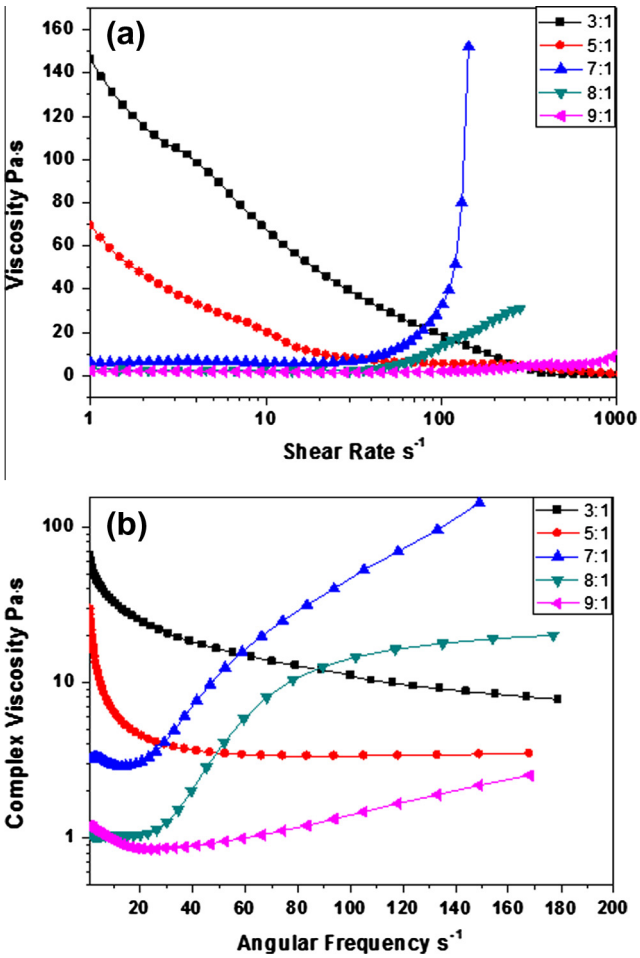

Fig. 5. (a) Viscosity *vs.* shear rate for PS–AA mass fraction 56% with different monomer molar ratios of St/AA dispersed in ethylene glycol, ratios: 3/1, 5/1, 7/1, 8/1, 9/1. (b) Complex viscosity *vs.* angular frequency for PS–AA mass fraction 56% with different monomer molar ratios of St/AA dispersed in ethylene glycol, ratios: 3/1, 5/1, 7/1, 8/1, 9/1. Dynamic frequency sweep at $T = 25$ °C, $\gamma = 200\%$.

The shear thinning phenomenon often occurs prior to the ST due to the formation of a two-dimensional layer structure at low shear rate. However, unlike other ST systems, a tiny ST behavior has been found before shear thinning in this work (Fig. 4a), which may be responded to the high charge density of the PS–AA nanospheres. Fig. 4b shows the complex viscosity *vs.* angular frequency for different mass fractions. It can be seen that the critical angular frequency decreased and the maximum complex viscosity increased as the mass fraction of PS–AA particles increased, which is resembled to the trend of viscosity curves under steady shear.

Based on the above results, it was found that the monomer molar ratio of styrene/acrylic acid exhibited high influence on the inner structure of the PS–AA nanospheres, which further affected the rheological properties of the STFs. In this work, the styrene/acrylic acid ratio was changed from 3/1 to 9/1 and Fig. 5a presents the relative static rheological properties. Interestingly, increasing of the acrylic acid in the PS–AA nanospheres was harmful for the ST effects. When the ratio was kept as 3/1, the viscosity curve showed a shear thinning behavior and the viscosity of the suspensions reduced to about 0.05 Pa s when the shear rate increased to 1000 s^{-1}. When the ratio changed from 3/1 to 5/1, there was still no ST effect and only the initial viscosity was decreased from 146 Pa s to 69.4 Pa s. However, as the ratio reached to 7/1, the initial viscosity reduced to 6 Pa s, and the viscosity exhibited a sharp increase once the shear rate reached to 50 s^{-1}, which was the typical characteristic of the STF. The maximum viscosity could reach to be as high as 152.2 Pa s. It can be concluded that increasing of the monomer ratio not only reduces the initial viscosity but also helps for the ST effect. Unfortunately, the ST effect was weakened with further increasing the monomer ratio. When the ratios were kept at 8/1 and 9/1, both products showed ST behavior. The initial viscosities and critical shear rates were similar to the ratio of 7/1. However, the maximum viscosity declined dramatically as the ratio rose. Therefore, under the optimum monomer ratio (in this work is 7/1), the final STF exhibited the best ST effect. Fig. 5b shows the complex viscosity *vs.* angular frequency curves for the 56 wt% STFs with PS–AA nanospheres which were synthesized under different monomer ratios. Similar to the steady shear mode, the oscillatory sweep curves also showed that the 7/1 ratio led to the highest ST effect, which indicated the STF had analogous rheological behavior in steady and oscillatory shear.

Besides the monomer ratio, the cross-link density also plays an important role in the inner structure of the PS–AA nanospheres. Here, the divinyl benzene (DVB) was introduced into the reaction system during the preparation of the PS–AA nanospheres to increase the cross-link density and the final nanospheres were defined as PS–AA–DVB-a%, in which the a% indicated the amount of the DVB. By keeping the monomer ratio of 8:1 as a constant, the PS–AA–DVB nanospheres were synthesized under varying the DVB component from 0.1% to 0.6%. After dispersing these PS–AA–DVB nanospheres into the EG solvent, the rheological properties

were investigated. As shown in Fig. 6a, in comparison with the PS–AA–DVB-0% based STF, the initial viscosity of the PS–AA–DVB-0.1% increased slightly and it exhibited a shear thinning behavior with increasing of the shear rate. As soon as the shear rate reached to 30 s^{-1}, the viscosity rapidly increased which indicates the presence of the ST effect. Although the increment was gentle, the maximum viscosity was similar to the PS–AA–DVB-0% based STF. With further increasing the DVB to 0.2%, the critical shear rate shifted slightly larger and the same to the maximum viscosity. Strangely, when the DVB reached to 0.3%, a strong ST effect was found and the suspensions exhibited a sharp increasing in viscosity at a small critical shear rate 7.8 s^{-1}. The maximum viscosity was up to 385.2 Pa s and this value was nearly 12 times larger than that of suspension with the corresponding PS–AA particles. However, when the amount of DVB was further increased to 0.4%, although the critical shear rate was similar to the PS–AA–DVB-0% based STF, the maximum viscosity was still larger and the increment was sharper. Too much DVB was useless for changing the structure characteristics of the PS–AA nanospheres, therefore the rheological curves for the PS–AA–DVB-0.5% and PS–AA–DVB-0.6% based STFs were similar to the PS–AA–DVB-0% based STF while the critical shear rates slightly increased. Fig. 6b presents the complex viscosity *vs.* angular frequency for PS–AA–DVB based STFs with different amounts of cross-linking monomer DVB. It can be seen that the changes in the rheological behavior under steady shear and oscillatory shear are the same, indicating the high credibility. Generally, the ST behaviors of the PS–AA–DVB nanospheres based STFs were highly dependent on the cross-link densities and the STFs with different critical shear rates and maximum viscosities could be alternatively obtained by varying the amount of the DVB. In addition, the best ST effect was achievable under the optimum condition.

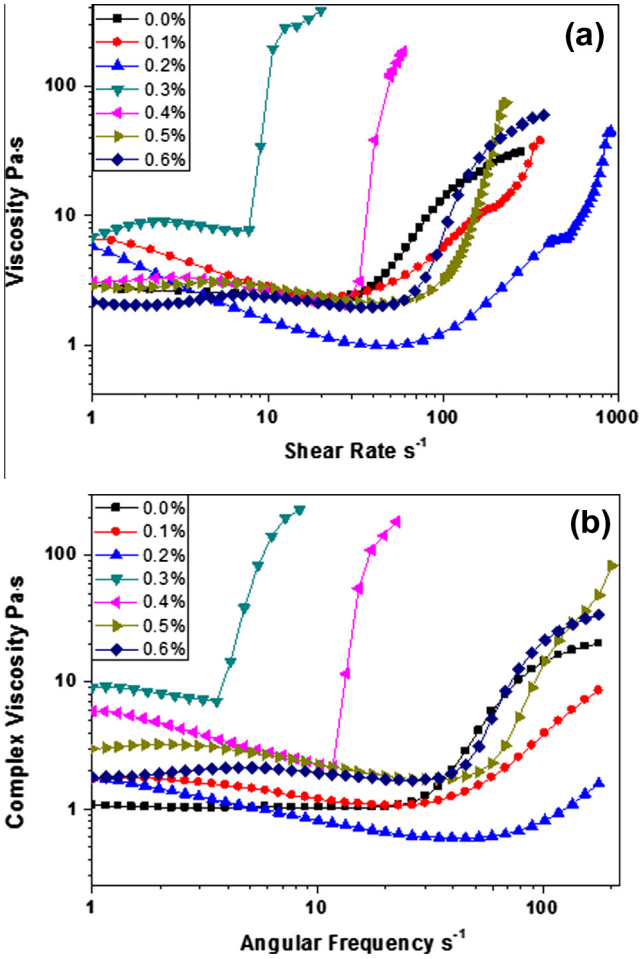

Fig. 6. (a) Viscosity *vs.* shear rate for STFs of the PS–AA–DVB particles dispersed in ethylene glycol with different amounts of cross-linking monomer DVB. (b) Complex viscosity *vs.* angular frequency for STFs of PS–AA–DVB particles dispersed in ethylene glycol with different amounts of cross-linking monomer DVB, Dynamic frequency sweeps at T = 25 °C, γ = 200%, ω = 56%.

The PS–AA based STF system provided relative higher severer ST behavior and higher critical shear rate than the STFs composed of inorganic silica or polymer PMMA particles [26,20], which enable them a wide practical application. Moreover, different from the past research, this work demonstrated a novel method to control the rheological properties of the final STFs by simply tuning the inner structure of the dispersing polymer nanospheres other than the traditional way of tuning the pH, surfactant, and ion strength [23,24]. Most importantly, it was found that the variation in the monomers ratio and the cross-linking reagent amount can alter the particle surface, particle hardness and shell thickness. These parameters were critical for determining the critical shear rate and the maximum viscosity of STF. Therefore, this method also supplied many useful experimental evidences for thoroughly understanding the ST mechanism.

3.3. Possible mechanism for the PS–AA nanospheres based STF

The PS–AA and PS–AA–DVB nanospheres were synthesized through soap-free emulsion polymerization method in the water solvent. Because the styrene is hydrophobic and the acrylic acid is hydrophilic, the oligomers of acrylic acid partly served as a kind of surfactant in the reaction. The final PS–AA nanospheres were somewhat as similar as the core–shell structure, but of course different from the typical core–shell structure, which can be further proved by the TEM images (Fig. SI 3). As-prepared PS–AA nanosphere had a PS-rich core and a PAA-rich shell, and the surface of the nanosphere was PAA. By changing the molar ratio of styrene/acrylic acid during the polymerizations, the composition of the core, shell and the surface of the particles would change, respectively. Under a small styrene/acrylic acid ratio, PS–AA nanosphere with a thicker shell and a smaller core would be obtained. The length of PAA chain in the surface of PS–AA nanosphere was relatively longer, thus the interaction among the adjacent particles was strong and the initial viscosity of the suspensions was very large. As the relative amount of styrene increased, the thickness of the PAA-rich shell and the length of the PAA chain in the surface decreased, which weakened the interaction among particles. Therefore, the initial viscosity of suspensions decreased quickly with increasing of the ratio of styrene/acrylic acid at the beginning. With further increasing of the styrene, the PAA chains in the surface were very short. PAA chain interaction among the nanospheres could no longer be considered, thus the change in the interaction among particles would not be obvious, and the initial viscosity of suspension no longer changed significantly.

For the PS–AA nanospheres synthesized at small styrene/acrylic acid ratio, no ST phenomenon was found under applying shear. There were two possible reasons: Firstly, at the very beginning, ST was suppressed by strong interaction among the PS–AA nanospheres. Secondly, the styrene is a rigid monomer, while acrylic acid is a flexible monomer. When the ratio was small, the PS-rich core was small and the PAA-rich shell was very thick. Due to the weak hardness of the nanospheres, the cluster of these nanospheres could not resist external imposed stress, thus no ST was found. In this system, the hardness of the PS–AA nanospheres was very important for the ST effects. To investigate the hardness of the particles, the PS–AA nanospheres synthesized with the ratio styrene/acrylic acid 3/1 and 9/1 were treated under ball milling for 24 h. As shown in Fig. 7, the PS–AA nanospheres with the ratio 3/1 showed a significant deformation after ball milling, while no defor-

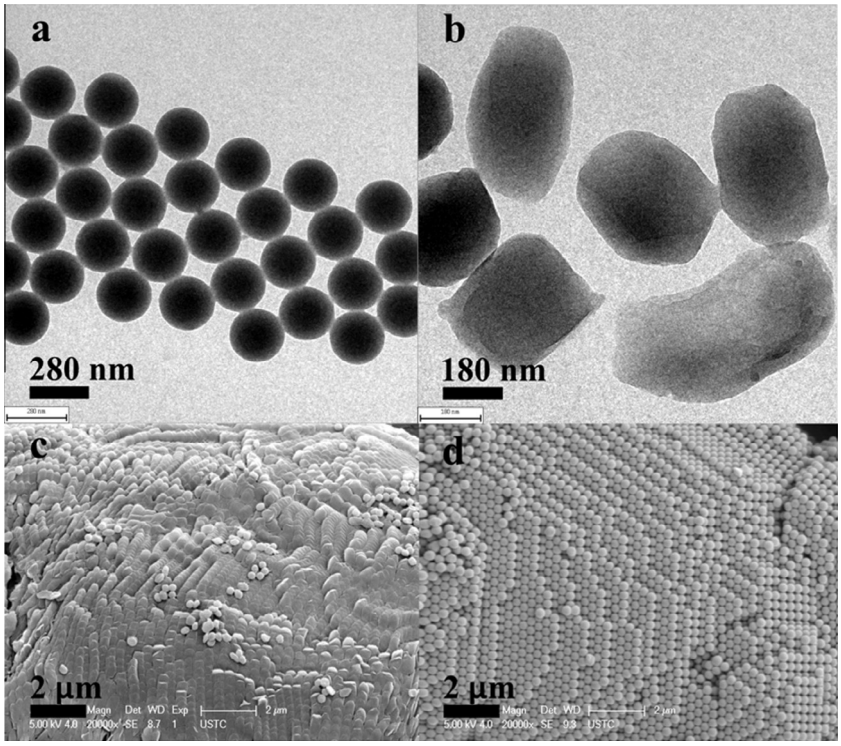

Fig. 7. TEM images of PS–AA particles synthesized at the ratio of St/AA = 3/1 before and after ball milling, before ball milling (a), after ball milling (b). SEM images of the PS–AA particles after ball milling with the molar ratio of the monomer St/AA = 3/1 (c) and 9/1 (d).

mation was found in nanospheres with the ratio 9/1, which still maintained a good spherical morphology. Clearly, with increasing of the styrene/acrylic acid ratio, the hardness of PS–AA nanospheres was significantly improved. When the ratio reached to a certain value, the suspension would exhibit ST behavior, therefore the hardness of the particles is an important factor on influencing the ST behavior of suspensions. However, when the ratio reached certain value (and then continue to increase), the amount of PAA in the surface would be reduced dramatically, which further led to the reduction in the carboxyl group. In this case, it was more difficult for hydrodynamic force to drive particles to form particle clusters due to the poor matching of the particles with the dispersion agent. As a result, a higher shear rate was needed to form the particle cluster and the formed cluster would be smaller. Therefore, the ST behavior occurred at a higher shear rate and the severity of shear thickening decreased.

Similarly, the hardness of the PS–AA–DVB nanospheres was also highly increased by increasing the cross-link densities, and thus the ST behavior of the final STFs based on the PS–AA–DVB nanospheres was stronger than non-cross-link ones. When the amount of the DVB was low, it mainly acted in the PS core of the nanospheres and greatly accelerated the polymerization of styrene. Some acrylic acid or acrylic acid oligomers were wrapped in the core, and hence the amount of PAA in the shell and in the surface would be reduced. In this case, the match of the particles with the dispersion agent would be poor, thus the critical shear rate shifted to larger value. Additionally, due to the cross-linking of the core, the hardness of particles increased, leading to a slight increase in ST effect. As the amount of DVB increased to 0.3%, both of the core and shell of particles were cross-linked and there would be a certain amount of PAA in the surface. In this point, the cluster could be formed much easier and was strong enough to resist the external shear stress, and therefore the suspensions exhibited a sharp increase in viscosity at a lower shear rate. The results further indicated that the suspension with the small ratio of styrene/acrylic acid exhibited no ST effect was a consequence of combination of the above two reasons and the hardness of particles plays an important role in the ST behavior. The cross-link in the surface of particles would increased with the further increasing of the amount of DVB, and the hydrophilicity of particles would be reduced, which led to the poor match between the PS–AA–DVB nanospheres and the dispersion agent. Therefore, the ST could only occur at an even higher shear rate and the severity decreased. The schematic illustration for influence of the styrene/acrylic acid ratio and the DVB cross-linking agent on the structure of the PS–AA nanospheres was showed in Scheme 1.

Under applying high shear rate on the concentrated suspensions, if the particles and dispersant agent have certain degree of matching, the particles will be pushed into stress-bearing clusters by hydrodynamic lubrication force, which produced by high shear rate. The viscosity of suspensions will increase due to these clusters and thus the ST phenomenon will appear in suspensions. Based on above results, we can draw three conclusions. Firstly, too strong interaction among the particles would prevent the occurrence of ST phenomenon and this result was in coincidence with the previous research [3]. Secondly, the hardness of suspended phase played an important role in the ST behavior. Even the particle clusters formed under hydrodynamic force, they still could not resist the external stress if the hardness of the particles was small. Therefore, no strong ST behavior exhibited in suspensions when subjected to a strong impact. Finally, the good match between the particles and the dispersant agent would facilitate the formation of the particle cluster produced by hydrodynamic lubrication forces.

In addition, with increasing of the styrene/acrylic acid ratio, the thickness of the shell of PS–AA nanospheres would reduce. In combination of the rheological properties and the structure characterization of the nanospheres, there would be an optimum particle structure for STF. In this work, it can be presumed that the nanosphere which has a hard core and a soft shell of a certain thickness would be contributed to the strong ST behavior. The soft shell would contribute to the lubrication hydrodynamic interaction,

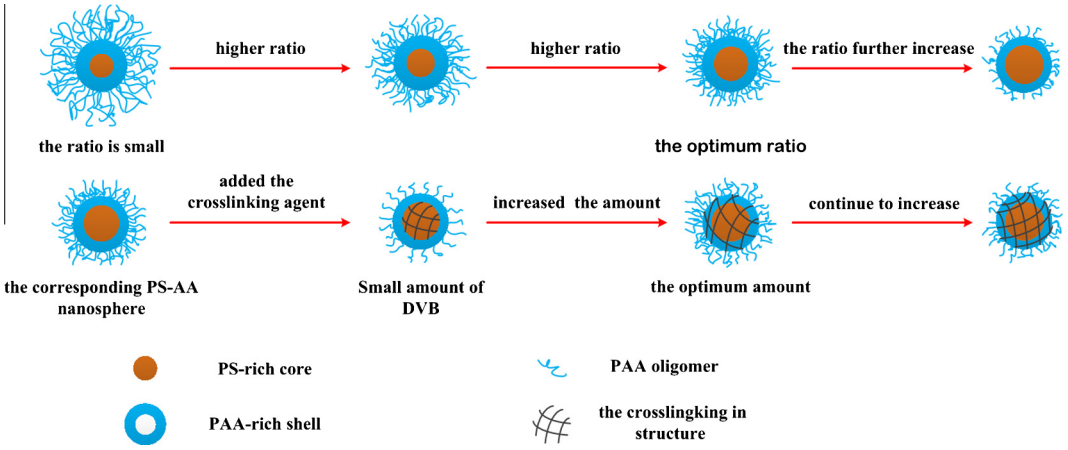

Scheme 1. Influence of the styrene/acrylic acid ratio and the cross-linking agent divinyl benzene on the structure of the PS–AA nanospheres.

therefore, it was easy for hydrodynamic force to aggregate particles to form particle clusters when the suspension was subjected to shear rate. The hard core of the nanosphere ensured the formed clusters could resist the external pressure. Here, the PS–AA nanospheres were treated under radiation to increase their hardness. Interestingly, the testing indicated that the treated PS–AA nanospheres based STF exhibited stronger ST effect than the non-treated one, which agreed well with the above analysis (Fig. SI 4). Based on the above work, it can be concluded that the ST effects were highly dependent on the inner structure of the dispersing nanospheres. By tuning the experimental parameters, the structure characteristics of the nanospheres were alternatively obtained which further helpful for the designation of the high performance STFs. Here, the detailed mechanism for the particles' structural dependent rheological behavior is still undergoing.

4. Conclusions

In this work, the nanospheres' structure dependence of the rheological properties of the STF was systematically studied using the poly(styrene–acrylic acid) (PS–AA) nanospheres as the dispersing particles. The structure characteristics of the PS–AA nanospheres were tunable by varying the monomer molar ratio of styrene/acrylic acid and the DVB. Based on the rheological tests of the final PS–AA nanospheres based STFs, an optimum styrene/acrylic acid ratio was found (7/1) and the maximum viscosity of the best STF was up to 152.2 Pa s as the mass fraction increased to 56%. Moreover, keeping other parameters as constant, when the DVB amount was increased to 0.3%, the maximum viscosity was up to 385.2 Pa s. The possible mechanism for the structure dependent rheological properties was carefully investigated and it was found that the ST effects were highly influenced by the surface charges and the particles' hardness, in which can be controlled by varying the monomer ratio of the precursor and the relative cross-link density. It was also proposed that if a nanosphere possessed a hard core and a soft shell of a certain thickness, their suspension would exhibit strong ST behavior. This work not only provides a good understanding of the particles' structure dependent ST behavior, but also supplies a new PS–AA system for the STFs.

Acknowledgments

Financial supports from the National Natural Science Foundation of China (Grant Nos. 11372301, 11125210) and the National Basic Research Program of China (973 Program, Grant No. 2012CB937500) are gratefully acknowledged.

Appendix A. Supplementary material

Supplementary data associated with this article can be found, in the online version, at http://dx.doi.org/10.1016/j.jcis.2013.09.020.

References

[1] R.L. Hoffman, Trans. Soc. Rheol. 16 (1972) 155–173.
[2] R.L. Hoffman, J. Colloid Interface Sci. 46 (1974) 491–506.
[3] H.A. Barnes, J. Rheol. 33 (1989) 329–366.
[4] X.Z. Zhang, W.H. Li, X.L. Gong, Smart Mater. Struct. 17 (2008) 035027.
[5] T.J. Kang, C.Y. Kim, K.H. Hong, J. Appl. Polym. Sci. 124 (2012) 1534–1541.
[6] Y.S. Lee, E.D. Wetzel, N.J. Wagner, J. Mater. Sci. 38 (2003) 2825–2833.
[7] R.L. Hoffman, Adv. Colloid Interface Sci. 17 (1982) 161–184.
[8] R.L. Hoffman, MRS Bull. 16 (1991) 32–36.
[9] L.B. Chen, M.K. Chow, B.J. Ackerson, C.F. Zukoski, Langmuir 10 (1994) 2817–2829.
[10] J. Bender, N.J. Wagner, J. Rheol. 40 (1996) 899–916.
[11] M.K. Chow, C.F. Zukoski, J. Rheol. 39 (1995) 33–59.
[12] B.J. Maranzano, N.J. Wagner, J. Chem. Phys. 117 (2002) 10291–10302.
[13] J.W. Bender, N.J. Wagner, J. Colloid Interface Sci. 172 (1995) 171–184.
[14] V.T. O'Brien, M.E. Mackay, Langmuir 16 (2000) 7931–7938.
[15] H.M. Laun, R. Bung, S. Hess, O. Hess, W. Loose, K. Hahn, E. Haedicke, R. Hingmann, F. Schmidt, P. Lindner, J. Rheol. 36 (1992) 743–787.
[16] M.C. Newstein, H. Wang, N.P. Balsara, A.A. Lefebvre, Y. Shnidman, H. Watanabe, K. Osaki, T. Shikata, H. Niwa, Y. Morishima, J. Chem. Phys. 111 (1999) 4827–4838.
[17] X. Cheng, J.H. McCoy, J.N. Israelachvili, I. Cohen, Science 333 (2011) 1276–1279.
[18] G. Bossis, J.F. Brady, J. Chem. Phys. 91 (1989) 1866–1874.
[19] W.H. Boersma, J. Laven, H.N. Stein, J. Colloid Interface Sci. 149 (1992) 10–22.
[20] W.Q. Jiang, Y.Q. Sun, Y.L. Xu, C. Peng, X.L. Gong, Z. Zhang, Rheol. Acta 49 (2010) 1157–1163.
[21] S.S. Shenoy, N.J. Wagner, Rheol. Acta 44 (2005) 360–371.
[22] M. Kamibayashi, H. Ogura, Y. Otsubo, J. Colloid Interface Sci. 321 (2008) 294–301.
[23] Y.L. Xu, X.L. Gong, C. Peng, Y.Q. Sun, W.Q. Jiang, Z. Zhang, Chin. J. Chem. Phys. 23 (2010) 342–346.
[24] G.V. Franks, Z.W. Zhou, N.J. Duin, D.V. Boger, J. Rheol. 44 (2000) 759–779.
[25] X.F. Sha, K.J. Yu, H.J. Cao, K. Qian, J. Nanopart. Res. 15 (2013) 1816(11).
[26] K.J. Yu, H.J. Cao, K. Qian, X.F. Sha, Y.P. Chen, J. Nanopart. Res. 14 (2012) 747(9).
[27] Y.S. Lee, N.J. Wagner, J. Rheol. 42 (2003) 199–208.
[28] H.G. Yang, C.Z. Li, H.C. Gu, T.N. Fang, J. Colloid Interface Sci. 236 (2001) 96–103.
[29] A. Zupancic, R. Lapasin, M. Zumer, Prog. Org. Coat. 30 (1997) 67–78.
[30] R.G. Egres, N.J. Wagner, J. Rheol. 49 (2005) 719–746.
[31] H.L. Yang, J.M. Ruan, J.P. Zou, Q.M. Wu, Z.C. Zhou, Y.Y. Xie, Chin. J. Chem. Phys. 22 (2009) 46–50.
[32] L.M. Zhang, T. Ma, J.L. Yang, Y. Huang, J. Inorg. Mater. 19 (2004) 1145–1150.
[33] A. Zupancic, M. Zumer, R. Lapasin, G. Torriano, Prog. Org. Coat. 30 (1997) 79–88.
[34] W.J. Frith, A. Lips, Adv. Colloid Interface Sci. 61 (1995) 161–189.
[35] E.B. Bagley, D.D. Christianson, J. Texture Stud. 13 (1982) 115–126.
[36] D.D. Christianson, E.B. Bagley, Cereal Chem. 60 (1983) 116–121.
[37] L. Chang, K. Friedrich, A. Schlarb, R. Tanner, L. Ye, J. Mater. Sci. 46 (2011) 339–346.
[38] Y. Otsubo, M. Fujiwara, M. Kouno, K. Edamura, Rheol. Acta 46 (2007) 905–912.
[39] X.L. Gong, Y.L. Xu, W. Zhu, S.H. Xuan, W.F. Jiang, W.Q. Jiang, J. Compos Mater. (2013) 1–17.

[40] D.P. Kalman, R.L. Merrill, N.J. Wagner, E.D. Wetzel, ACS Appl. Mater. Interfaces 1 (2009) 2602–2612.
[41] B.J. Maranzano, N.J. Wagner, J. Chem. Phys. 114 (2001) 10514–10527.
[42] E. Brown, H.J. Zhang, N.A. Forman, B.W. Maynor, D.E. Betts, J.M. DeSimone, H.M. Jaeger, Phys. Rev. E. 84 (2011) 031408.